

Generalized multipartite entropic uncertainty relations: theory and experiment

Zhao-An Wang^{a,b,1}, Bo-Fu Xie^{c,1}, Fei Ming^{c,1}, Yi-Tao Wang^{a,b,1}, Dong Wang^{a,c,2}, Yu Meng^{a,b,2}, Zheng-Hao Liu^{a,b}, Jian-Shun Tang^{a,b,d,2}, Liu Ye^c, Chuan-Feng Li^{a,b,d,2}, Guang-Can Guo^{a,b,d}, and Sabre Kais^e

^aCAS Key Laboratory of Quantum Information, University of Science and Technology of China, Hefei 230026, People's Republic of China; ^bCAS Centre For Excellence in Quantum Information and Quantum Physics, University of Science and Technology of China, Hefei 230026, People's Republic of China; ^cSchool of Physics & Optoelectronic Engineering, Anhui University, Hefei 230601, People's Republic of China; ^dHefei National Laboratory, University of Science and Technology of China, Hefei 230088, People's Republic of China; ^eDepartment of Chemistry, Department of Physics, and Purdue Quantum Science and Engineering Institute, Purdue University, West Lafayette, IN 47907, USA

This manuscript was compiled on July 27, 2022

Entropic uncertainty relation (EUR) plays a vital role in quantum information theories by demonstrating the intrinsic uncertainty of nature from the information-theoretic perspective. A tighter lower bound for uncertainty relations facilitates more accurate predictions of measurement outcomes and more robust quantum information processing. However, meaningful EURs in multipartite scenarios are yet to be identified. In this study, we derived a generalized EUR (GEUR) for the measurement of multiple observables in arbitrary many-body systems. The corresponding GEUR bound is shown to be tighter than Renes Boileau *et al.*'s bound when applied in a tripartite scenario. We experimentally tested the GEUR with a four-photon entangled state in an optical platform. We demonstrated that GEUR provide a tighter lower bound of the quantum-secret-key rate, which can readily accelerate practical quantum key distribution protocols. By providing a close peek at the nature of uncertainty, our results may find broad applications in the security analysis of quantum cryptography.

Uncertainty relation | Quantum information | Quantum cryptography

The Heisenberg (1) uncertainty is capable of bounding the uncertainties of measurement results of two incompatible observables. Its advent has revolutionized people's acknowledgements of the quantum world. It can be expressed by a canonical variance-based formula; in a given system ρ , the uncertainty of two observables \hat{R} and \hat{K} can be expressed as (2, 3) :

$$\Delta_\rho \hat{R} \cdot \Delta_\rho \hat{K} \geq \frac{1}{2} \left| \left\langle \left[\hat{R}, \hat{K} \right] \right\rangle_\rho \right|. \quad [1]$$

Despite its success, the Heisenberg uncertainty principle inevitably results in the problem of state dependence (4). To eliminate this drawback, Deutsch (5) introduced the concept of Shannon entropy from classical information theory as a measurement of quantum uncertainty, the so-called entropic uncertainty relation (EUR). Furthermore, Kraus (6) and Massen and Uffink (7) developed Deutsch's work and strengthened the lower bound of the total entropy for two incompatible measurements on a single system, yielding the following celebrated result reads:

$$H(\hat{R}) + H(\hat{K}) \geq -\log_2 c(\hat{R}; \hat{K}) =: q_{\text{MU}}, \quad [2]$$

where $c(\hat{R}; \hat{K}) = \max_{i,j} |\langle \varphi_i | \phi_j \rangle|^2$ denotes the maximum overlap between the eigenstates of chosen observables \hat{R} and \hat{K} on subsystem A , i.e., $|\varphi_i\rangle$ and $|\phi_j\rangle$.

The EUR perfectly combines quantum mechanics and information theory, and the new derived entropic lower bound only depends on the complementarity of the observables to be measured. However, the original form only applies to a single system. Renes *et al.* (8) and Berta *et al.* (9) considered EURs in composite systems and proposed a quantum-memory-assisted entropic uncertainty relation (QMA-EUR). In detail, the entropic uncertainty of system A can be predicted with a tighter bound when it is correlated with memory system B ; the mathematical form is as follow :

$$S(\hat{R}|B) + S(\hat{K}|B) \geq -\log_2 c(\hat{R}; \hat{K}) + S(A|B), \quad [3]$$

where $S(\cdot)$ denotes the von Neumann entropy, the term $S(\hat{R}|B) = S(\rho_{\hat{R}B}) - S(\rho_B)$ denotes the conditional en-

Significance Statement

Entropic uncertainty relations (EURs) are both cornerstones of the contemporary information-theoretic interpretation of quantum theory and vital tools for the security analysis of quantum cryptography. Despite several related advances in this direction, a generalization of GEUR for many-body systems does not exist. In this study, we show how a strong GEUR can be constructed for arbitrary many subsystems. The relation is strong in the sense that it gives tighter bounds for entropic analysis of few-body systems surpassing the best previously known results, and it is capable of improving the lower bound of quantum-secure-key rate in practical quantum key distribution. Furthermore, the advantage of our proposed GEUR and its application in quantum cryptography is directly confirmed in a multi-photon experiment.

D.W. conceived the study; Y.M. designed the experiment; Z.-A.W. performed the experiment with the assistance of Y.-T.W., Z.-H.L. and Y.M.; B.-F.X. and F.M. derived the theoretical results. Y.L., S.K. and D.W. supervised the theoretical part of the project; J.-S.T., C.-F.L. and G.-C.G. supervised the experimental parts of the project. All authors contributed to the writing of the manuscript and discussed the results.

The authors declare that they have no competing interests.

¹Z.-A.W., B.-F.X., F.M. and Y.-T.W. contributed equally to this work.

²To whom correspondence should be addressed. E-mail: dwang@ahu.edu.cn (D.W.), mengyu23@mail.ustc.edu.cn (Y.M.), tjs@ustc.edu.cn (J.-S.T.), cflil@ustc.edu.cn (C.-F.L.)

trophy after applying unilateral measurement \hat{R} on subsystem A (the same for observable \hat{K}). Meanwhile the post-measurement state is :

$$\rho_{\hat{R}B} = \sum_i (|\varphi_i\rangle\langle\varphi_i| \otimes \mathbb{I}) \rho_{AB} (|\varphi_i\rangle\langle\varphi_i| \otimes \mathbb{I}). \quad [4]$$

The conditional entropy $S(A|B)$ represents the correlation of subsystem B owned by its memory system A . If quantum memory B is absent, $H(\hat{R}) + H(\hat{K}) \geq q_{\text{MU}} + S(A)$ maintains, meaning that a tighter bound is attained due to $S(A) \geq 0$, in sharp comparison with the Maassen and Uffink's single subsystem bound in Eq. [2] where $S(A) = 0$ (6, 7). The QMA-EUR elucidates from an information-theoretic perspective that, if subsystems A and B are maximally entangled, the measurement results of subsystem A can be accurately predicted by subsystem B . Furthermore, Adabi *et al.* (10) introduced the Holevo quantity and mutual information in the study of EUR and provided an improved the lower bound of Eq. [3], which is the tool we employ to build our generalized framework.

Notably, the QMA-EUR, although initially developed to improve the predictive accuracy of the quantum uncertainty principle, is also a pillar for quantum information processing. It has shown profound affiliation in building the entanglement criterion (11–13), certifying quantum randomness (14), deriving quantum steering inequality (15–17), executing security analysis of the quantum communication (18–21), etc. Moreover, it directly reflects the security of quantum key distribution (QKD): a tighter EUR guarantees a higher quantum-secure-key (QSK) rate and hence signifies higher security to QKD (19). In this sense, deriving tighter EUR bounds is paramount. Thus, several scientists have proposed different techniques in the regime of two-measurement of bipartite systems (22–28), as well as conducted experimental researches in all-optics (29–31), neutron (32), and diamond (33) platforms. Actually, as a critical application in the security analysis of QKD, EURs need not only the version of simple two- or three-particle systems but also the more general many-body version. It is only recently that the EUR of multi-observable scenario has been developed (34, 35), and Renes and Boileau (8) significantly proposed a tripartite EUR as:

$$S(\hat{R}|B) + S(\hat{K}|C) \geq q_{\text{MU}}. \quad [5]$$

Its core difference with Eq. [3] is that, on the left-hand side, Eq. [5] inequality quantifies the lower bound of the uncertainty of the unilateral measurement on subsystems B and C . While the term q_{MU} is the same as in Eq. [3].

Finding a generalized communication bound that suits arbitrary multiple nodes is at the heart of constructing a quantum network. Contrary to all aforementioned EURs, our work is a generalized version; first, we derive a tighter tripartite QMA-EUR bound than Renes–Boileau's bound (Eq. [3]), and then obtain a generalized

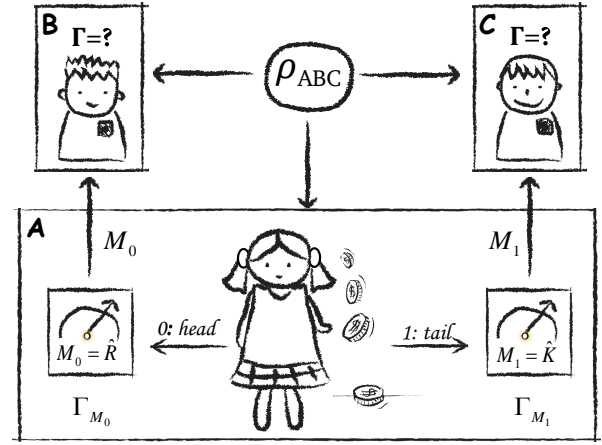


Fig. 1. Schematic illustrating the uncertainty game in a tripartite quantum system. First, there is a tripartite state ρ_{ABC} , and then subsystem A is transmitted to Alice, whereas subsystems B and C are transmitted to Bob and Charlie respectively. Second, Alice performs either \hat{R} or \hat{K} measurement observables on A and she has a measure outcome Γ , and then announces the measurement choice M to Bob and Charlie. When both Bob and Charlie predict Γ with the bound of guess uncertainty q_{MU} , they win this game.

EUR (GEUR) for multi-measurement in the presence of arbitrary multipartite systems. Next, we devise a photonic platform that can experimentally generate four-qubit Greenberger–Horne–Zeilinger (GHZ) entanglement states and arbitrary multilateral measurements. Assisted by this platform, we confirm the tightness of our GEUR for a four-partite system. Finally, we introduced an application of our tripartite QMA-EUR by improving the lower bound of QSK by adopting three-qubit Werner states on the same platform.

Results

Tighter multipartite GEUR.

Adapted from Renes–Boileau's result Eq. [5], we first proposed a tighter tripartite QMA-EUR by illustrating an uncertainty game among three correlated subsystems. To introduce this game, we plot a diagram in Fig. 1: Three participants, Alice, Bob and Charlie, share a tripartite state ρ_{ABC} prepared *in priori*. At the beginning of the game, Alice randomly selects one of two observables (\hat{R} and \hat{K}) and obtains a measurement outcome Γ . Later, Alice notifies her measurement's choice to Bob or Charlie according to the choice of the observable. The players would win the game if Bob or Charlie correctly guess the outcome of Alice's measurement. Our proposed QMA-EUR gives an upper bound of the winning probability for the guessing game. Formally, it is stated in the following theorem:

Theorem 1. An improved tripartite EUR in terms of the entropy and conditional entropy of subsystems and the Holevo quantities can be stated by:

$$S(\hat{R}|B) + S(\hat{K}|C) \geq q_{\text{MU}} + \max \{0, \Delta\}, \quad [6]$$

with

$$\Delta = S(A) - [\mathcal{I}(\hat{R} : B) + \mathcal{I}(\hat{K} : C)], \quad [7]$$

where $S(A) = -\sum_i \lambda_A^i \log_2 \lambda_A^i$ with λ_A^i being the i -th eigenvalue of state ρ_A and $\mathcal{I}(\hat{R} : B) = S(\rho_{\hat{R}}) + S(\rho_B) - S(\rho_{\hat{R}B})$ and $\mathcal{I}(\hat{S} : C) = S(\rho_{\hat{K}}) + S(\rho_C) - S(\rho_{\hat{K}C})$ denote the Holevo quantities, which means the upper bound of Bob's accessible information about Alice's measurement results. One can easily find that our bound will be tighter than that in Eq. [5] if $\Delta > 0$. When $\Delta \leq 0$, our result will naturally recover Renes–Boileau's result. The proof is presented in the Materials and Methods section.

Technically, compared to tripartite scenarios, a EUR of multiple measurements in multiparty systems is on-demand in realistic many-body-based quantum information processing, which is deemed as a general case. In this sense, we next focus on addressing this issue and presenting a GEUR with respect to the multiple measurement architecture.

Theorem 2. A GEUR for measurements of multiple observables in the context of multipartite systems can be expressed as

$$\sum_{i=1}^N S(\hat{O}_i | B_i) \geq -\frac{\sum_{i \neq j, i=1}^N \log_2 c(\hat{O}_i; \hat{O}_j)}{N-1} + \max\{0, \Delta_N\}, \quad [8]$$

with

$$\Delta_N = \frac{N}{2} S(A) - \sum_{i=1}^N \mathcal{I}(\hat{O}_i : B_i), \quad [9]$$

where \hat{O}_i denotes the i -th measurement on subsystem A , and B_i denotes the i -th memory except subsystem A in multi-particle subsystem comprising $AB_1B_2B_3B_4 \cdots B_N$.

As the number of observable N increases, the calculations' overlapping terms $c(\hat{O}_i, \hat{O}_j)$ become more complex as it involves taking the maximum for all bases of each corresponds observables. We show that, fortunately, this conundrum can be solved with the aid of mutually unbiased bases (MUBs), wherein all maximums will depend on only the dimensions of the systems. We assume there are two groups of orthogonal bases $\{|\varphi_a\rangle\}_{a=1,2,\dots,d}$ and $\{|\phi_b\rangle\}_{b=1,2,\dots,d}$ in a d -dimensional Hilbert space. Generally, the two groups of orthogonal bases are termed as MUBs if

$$|\langle \varphi_a | \phi_b \rangle| = \frac{1}{\sqrt{d}} \quad [10]$$

holds for all a and b (36). Obviously, we have $c(\hat{O}_i; \hat{O}_j) \equiv 1/d$ ($i \neq j$) if a group of incompatible observables with MUBs ($\hat{O}_1, \hat{O}_2, \dots, \hat{O}_N$) are taken as the measurement objects. In fact, two-dimensional Pauli-observable measurements are regarded as perfect MUBs in realistic quantum information processing.

To test our result, we here choose the canonical two-dimensional Pauli observables $\hat{\sigma}_x$, $\hat{\sigma}_y$ and $\hat{\sigma}_z$ as measurement objects in several four-qubit systems ρ_{ABCD} . In this case, we have $c(\hat{\sigma}_i, \hat{\sigma}_j) \equiv 1/2$. In addition, although Renes–Boileau's EUR is only suitable for tripartite system, herein we can rewrite it to derive an EUR for a quadruple scenario

$$S(\hat{R}|B) + S(\hat{K}|C) + S(\hat{Q}|D) \geq \mathcal{B}_{MU} := U_{RB}, \quad [11]$$

where

$$\mathcal{B}_{MU} = \frac{q_{MU1} + q_{MU2} + q_{MU3}}{2}, \quad [12]$$

$$q_{MU1} = -\log_2 c(\hat{R}; \hat{K}),$$

$$q_{MU2} = -\log_2 c(\hat{R}; \hat{Q}), \quad [13]$$

$$q_{MU3} = -\log_2 c(\hat{K}; \hat{Q}).$$

For $\hat{\sigma}_x$, $\hat{\sigma}_y$ and $\hat{\sigma}_z$ as the three-measurement, one can easily get $\mathcal{B}_{MU} = \frac{3}{2}$. By applying our result to three-measurement cases, a tighter bound can be obtained from the following relation

$$S(\hat{R}|B) + S(\hat{K}|C) + S(\hat{Q}|D) \geq \mathcal{B}_{MU} + \max\{0, \Delta_3\} \quad [14]$$

with

$$\Delta_3 = \frac{3}{2} S(A) - [\mathcal{I}(\hat{R} : B) + \mathcal{I}(\hat{K} : C) + \mathcal{I}(\hat{Q} : D)]. \quad [15]$$

Experiment.

To experimentally demonstrate the improvement of our bound compared with Renes–Boileau's bound, signified by the non-zero quantity Δ_3 in Eq. [14], we prepared four-qubit GHZ states as the testbed family of a multipartite system from two polarization-entangled photons pairs. The correspondence between the computational bases and photonic polarization states read $|0\rangle \sim |H\rangle$, $|1\rangle \sim |V\rangle$, with $|H\rangle$ and $|V\rangle$ denoting the horizontal and vertical polarization states of photon, respectively. As depicted in Fig. 2, two beam-like entangled photon pairs centered at the wavelength of 808 nm were generated via the spontaneous parametric down-conversion process by pumping two type-II β -barium borate (BBO) crystals sandwiches (37), where the pumping laser is the femtosecond pulsed laser centered at 404 nm with the repetition rate of 76 MHz. After compensating for the spatial and temporal walkoff by the birefringent crystals, two-qubit entangled source were prepared in the Bell state $|\Phi^+\rangle = (|HH\rangle + |VV\rangle)/\sqrt{2}$ with high fidelity above 99.0%. Then, the photons at four paths was filtered by 3-nm band-pass filters and coupled into single-mode fibers. The polarization states of the photons were maintained by four pairs of half-wave plates before and after the fiber to revert the unwanted polarization rotation induced by the fibers.

To prepare the 4-qubit GHZ entangled state, we took one photon from each of the entangled photon pair

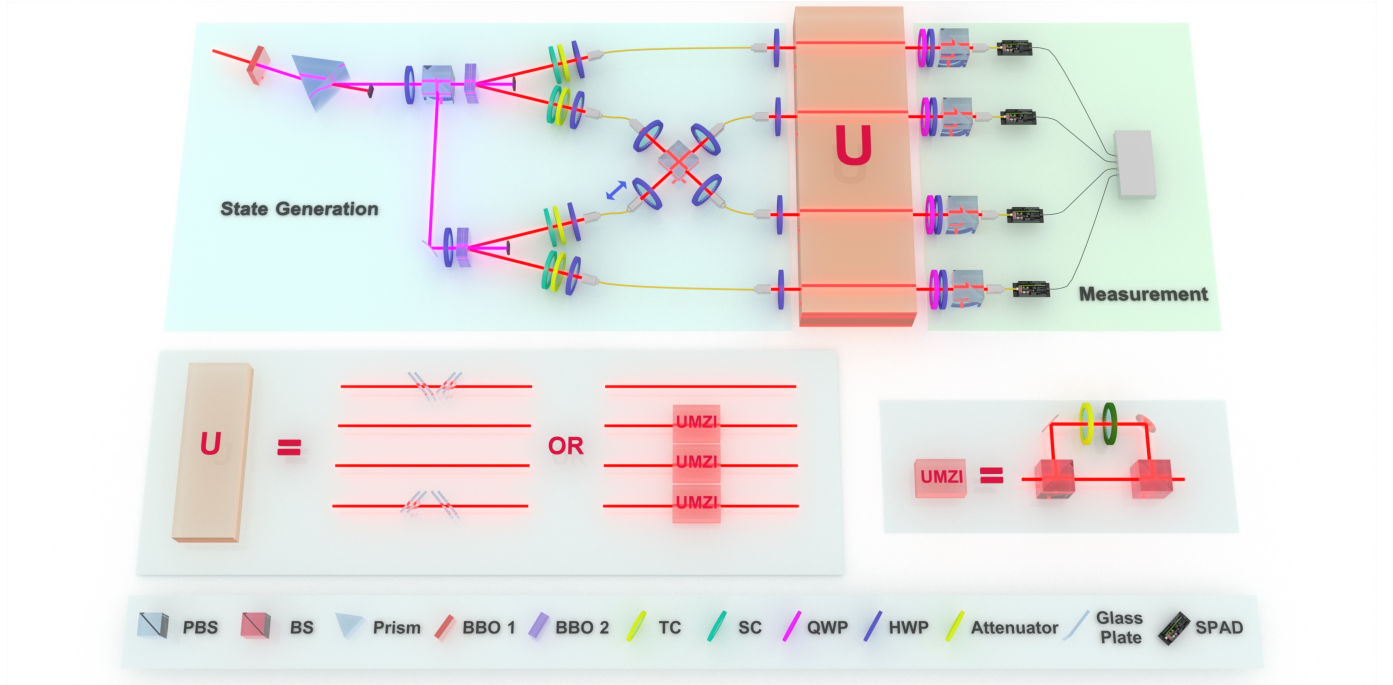


Fig. 2. Experimental setup for GHZ state. In the state preparation stage, two pairs of maximally entangled photons were generated by pumping nonlinear crystals with pulsed ultraviolet lasers. Two photons from each pair were interfered on a PBS to generate a four-photon GHZ state conditioned on coincidence counting. The HWPs before and after the single-mode fibers were used to maintain the state polarization. In the evolution stage, denoted by U , the four-photon GHZ state was further transformed to GHZ-like states Eq. [17] using tilted glass plates or Werner states Eq. [23] using an UMZI. In the measurement stages, the four photons underwent polarization analysis and coincidence counting. BS: beam splitter; TC(SC): temporal (spatial) compensator; QWP: quarter-wave plates; IF: interference filter; SPAD: single-photon avalanche detector.

to encounter at a polarizing beam splitter (PBS). The PBS transmits $|H\rangle$ -polarized photons and reflects $|V\rangle$ -polarized photons, respectively, so only two incident photons with the same polarization can be output coincidentally from different ports. We selected the events via four-fold coincidence photon counting detected at each output port simultaneously, and the PBS acted as a parity operator $|HH\rangle\langle HH| + |VV\rangle\langle VV|$ (38). The successful postselection projected the output state onto the four-qubit GHZ state:

$$|\text{GHZ}^4\rangle = \frac{1}{\sqrt{2}}(|HHHH\rangle + |VVVV\rangle)_{ABCD}, \quad [16]$$

with a probability of $\frac{1}{2}$. We have adjusted carefully the length of optical paths before the PBS to ensure the maximal multiple-photon interference visibility and employed a tiltable quarter-wave plate (QWP) oriented at 0° at one photon path to compensate the relative phase between the two terms of Eq. [16]. As the result, the experimentally prepared four-photon state shows the state-witness of 95%. The imperfection of state preparation can be attributed to the decoherence caused by polarization or phase difference, small misalignments in spatial modes, and the residual spectrum difference between the interfered photons. Furthermore, we expanded the family of prepared states by inserting groups of Brewster windows to adjust the relative amplitude of $|H\rangle$ and $|V\rangle$ -polarized wavefunction, which produces the set of experimentally

amenable states with different parameters of θ , after a re-normalization, to become:

$$|\text{GHZ}^4(\theta)\rangle = \cos\theta |HHHH\rangle + \sin\theta |VVVV\rangle. \quad [17]$$

Finally, we used four groups of polarization analysis devices, consisted by a QWP, an HWP and a PBS, to perform full sets of projective measurements.

We used quantum state tomography on various subsystems to deduce their density matrices and the corresponding von Neumann entropies. In particular, the Holevo quantities were calculated against the conditional quantum-classical state after the measurement of a specific observable has taken place. The results for testing the strong multipartite EUR are illustrated in Fig. 3. Both the theoretical left-hand side value of Eq. [14] and the Renes–Boileau’s bound, \mathcal{B}_{MU} , remain independent of the state parameter, the values are 2 and $\frac{3}{2}$, respectively. Experimentally, we measured the sum of conditional entropies, $S(\hat{R}|B) + S(\hat{K}|C) + S(\hat{Q}|D)$ on the left-hand side of Eq. [14] as all close to but slightly above 2. This slight difference is due to the small deviation of our experimental state from the ideal state given by Eq. [17]. We see that Renes–Boileau’s bound is not tight anywhere for this testbed family of states. However, the proposed multipartite EUR significantly improves the situation; the additional experimental term Δ_3 on the right-hand side of Eq. [14] is nonvanishing for all but one parameter choice $\theta = \frac{\pi}{4}$, and for the product state $\theta = 0$, it becomes $\frac{1}{2}$,

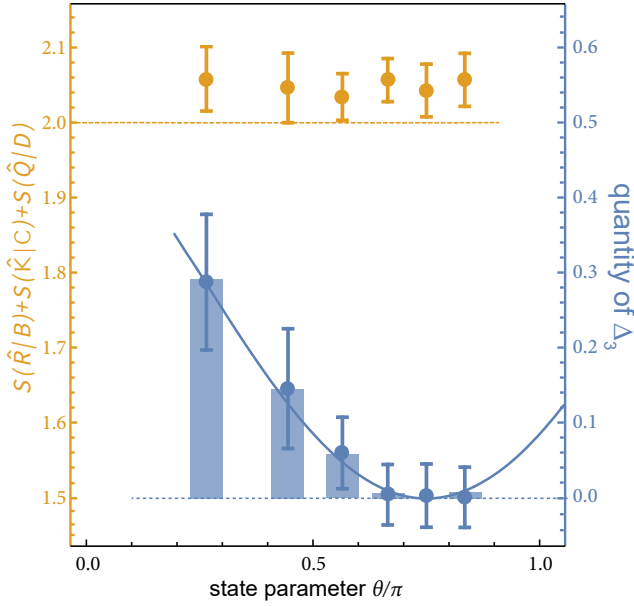


Fig. 3. Experimental certification of the tightness of our bound. The yellow dots are the experimental value of the left-hand side of Eq.[6], the quantity of $S(\hat{R}|B) + S(\hat{K}|C) + S(\hat{Q}|D)$, which is identically equal to constant 2 regardless of the state parameter θ . The blue points are the non-zero parts of Δ_3 which vary as θ changes. The corresponding histograms illustrate the improvement of our bound compared with the Renes–Boileau’s bound where $B_{MU} \equiv \frac{3}{2}$. The error bars denoting the 1σ standard deviation are deduced by assuming Poissonian counting statistics.

making our bound tight. Experimentally, we observed a maximum of $\Delta_3 = 0.323$ due to the limited extinction ratio of the Brewster window array. The results demonstrated a clear improvement by our bound of uncertainty from the Renes–Boileau’s bound.

Application to quantum key distribution.

Our tighter bound of uncertainty should be of fundamental relevance to the security analysis of QKD protocols in practical many-body systems. Particularly, we can focus on improving the lower bound of the QSK rate via our tighter bound for tripartite QMA-EUR. Regarding two honest participants (say, Alice and Bob), who are sharing a key by communicating over a public channel in the QKD processing, the key is secret to any third-party eavesdropper (eg., Dave). Notably, the quantity of key K that can be extracted by Alice and Bob is lower bounded by (39):

$$K \geq S(\hat{K}|D) - S(\hat{K}|B). \quad [18]$$

In the eavesdropper-existing communication process, Dave (eavesdropper) prepares a quantum state ρ_{ABD} ; and sends subsystems A and B to Alice and Bob respectively while keeping D . By connecting with Renes–Boileau’s bound shown as $S(\hat{R}|B) + S(\hat{K}|D) \geq q_{MU}$ in Eq. [5], we can derive

$$K \geq q_{MU} - S(\hat{R}|B) - S(\hat{K}|B). \quad [19]$$

On account of the fact that $S(\hat{R}|B) \leq S(\hat{R}|\hat{R}')$ and $S(\hat{K}|B) \leq S(\hat{K}|\hat{K}')$, we thus obtain the following inequality (29)

$$K^* \geq q_{MU} - S(\hat{R}|\hat{R}') - S(\hat{K}|\hat{K}'). \quad [20]$$

Based on Eqs. [6] and [19], for a the unilateral measurement, the new lower bound of the QSK rate can be derived into

$$K_{LB} \geq q_{MU} + \max\{0, \Delta\} - S(\hat{R}|B) - S(\hat{K}|B). \quad [21]$$

As is known that the measurement is unable to degrade the system’s entropy. Hence, for a bilateral measurement, the new bound of the QSK rate is as follow:

$$K_{LB}^* \geq q_{MU} + \max\{0, \Delta\} - S(\hat{R}|\hat{R}') - S(\hat{K}|\hat{K}'). \quad [22]$$

Owing to the additional item $\max\{0, \Delta\} \geq 0$, which means that the QSK rate bound we obtain shall be tighter than that attained by Berta *et al.* In this sense, we say that our lower bound is capable of efficiently improve the security of QKD protocols.

To clearly demonstrate our improvement in QSK rate in the current scenarios, we resort to a class of Werner states to derive the improvement of QSK rate. For simplicity, we experimentally prepare the system’s state as a three-photon Werner state, which is expressed by:

$$\rho_W(p) = p |\text{GHZ}^3\rangle \langle \text{GHZ}^3| + \frac{(1-p)}{8} I, \quad [23]$$

where $|\text{GHZ}^3\rangle = (|HHH\rangle + |VVV\rangle)/\sqrt{2}$ denotes the three-qubit GHZ state and I is the maximally mixed state. To prepare the Werner state, we replaced the Brewster

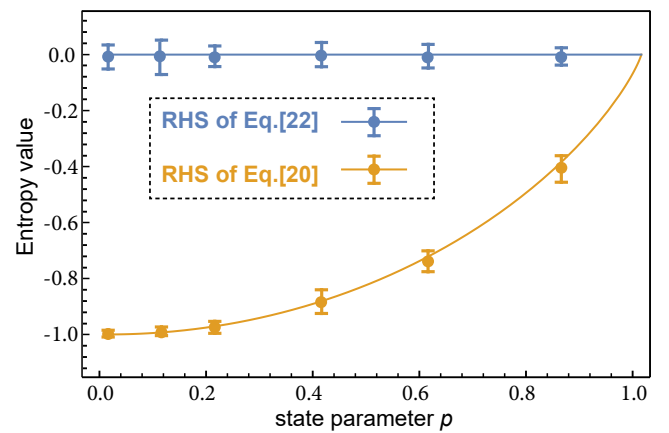


Fig. 4. Improved lower bound of QSK rate. The blue dots are the experimental results of the QSK rate of different Werner states (right-hand side of Eq. [22]), whereas the yellow dots (consistent with the theoretical yellow lines) represent the experimental results of the right-hand side of Eq. [20]. The error bars denoting the 1σ standard deviation are deduced by assuming Poissonian counting statistics.

windows in each path with an unbalanced Mach–Zehnder interferometer (UMZI) in the experimental setup (see Fig. 2) and removed one of the PBS in the measurement stage of the photon C to use it as a trigger photon. The variable attenuator in the interferometer allowed to adjust the mixing parameter p . The length difference between the two arms of each UMZI was roughly 0.8 m, and the coincidence interval was set to 0.8 ns to reject all events where some photons propagated through the long arm and the others through the short arm.

Fig. 4 shows the improvement of the QSK rate's lower bound with bilateral measurements. The scenario can be described as the subsystems A, B are sent to Alice and Bob respectively, and the eavesdropper (Dave) keeps D . For simplicity, we limit both Alice and Bob to employ σ_y and σ_z measurements as the observables respectively. The new bound derived from our multipartite EUR surpasses the best previous result; in the limit of $p \rightarrow 0$ the improvement becomes as large as 1. The experimental results, in excellent agreement with the theoretical prediction, clearly demonstrated the potential of our proposed EUR in implementing more efficient practical QKD using the existing infrastructure.

Discussion

In this study, we originally derived a GEUR for measurements of multiple observables under a multipartite architecture, which belongs to a universal case. As some illustrations to support our results, we choose three two-dimensional Pauli measurements σ_x , σ_y and σ_z as the incompatibility to experimentally measure within a various four-qubit GHZ states. It turns out that the GEUR always holds in all cases, and our corresponding lower bound is tighter than the previous ones. As a final remark, we highlighted that the GEUR can be applied to obtain a tighter bound of the QSK rate both theoretically and experimentally. Thus, we claim that our observation could offer more profound insight into entropy-based uncertainty relations for multi-measurement in the presence of arbitrary multipartite systems, and is thought to be essential to boost the security of realistic QKD protocols.

Going beyond the previous results, our work shows that the GEUR clearly supports the improvement of the QSK rate bound in practical QKD protocols, which is fundamentally beneficial to enhance the security of prospective quantum communication networks. Our work paves a pathway for addressing the preparation uncertainty of multiple measurements in many-body systems, including arbitrary incompatible measurements. The result lays also the foundations for the exploration of more complex, higher-dimensional measurements by state-of-the-art entropy-based information theories. An important next step towards applications for GEUR such as quantum cryptography, quantum randomness, quantum steering and quantum metrology, is a fertile and promising direction in quantum information sciences.

Materials and Methods

In this section, we provide detailed proofs of the theorems in the main text.

Proof of the Theorem 1 in the main text.—Considering the left item of the inequality [5], we can attain

$$S(\hat{R}|B) + S(\hat{K}|C) = H(\hat{R}) - \mathcal{I}(\hat{R} : B) + H(\hat{K}) - \mathcal{I}(\hat{K} : C), \quad [24]$$

and there is

$$H(\hat{R}) + H(\hat{K}) \geq q_{\text{MU}} + S(A), \quad [25]$$

as aforementioned. Substituting Eq. [25] into Eq. [24], the inequality becomes

$$S(\hat{R}|B) + S(\hat{K}|C) \geq q_{\text{MU}} + S(A) - [\mathcal{I}(\hat{R} : B) + \mathcal{I}(\hat{K} : C)]. \quad [26]$$

Combining Eqs. [5] and [25], taking a maximum between $S(A) - [\mathcal{I}(\hat{R} : B) + \mathcal{I}(\hat{K} : C)]$ and zero, we obtain the stronger result shown as Eq. [6].

Proof of the Theorem 2 in the main text.—We can write $N(N-1)/2$ inequalities analogous to Eq. [6] for N -observable measurements and an $N+1$ -party system $\rho_{AB_1B_2B_3B_4\cdots B_N}$ as

$$\begin{aligned} S(\hat{\mathcal{O}}_1|B_1) + S(\hat{\mathcal{O}}_2|B_2) &\geq -\log_2 c(\hat{\mathcal{O}}_1; \hat{\mathcal{O}}_2) + S(A) \\ &\quad - [\mathcal{I}(\hat{\mathcal{O}}_1 : B_1) + \mathcal{I}(\hat{\mathcal{O}}_2 : B_2)], \\ S(\hat{\mathcal{O}}_1|B_1) + S(\hat{\mathcal{O}}_3|B_3) &\geq -\log_2 c(\hat{\mathcal{O}}_1; \hat{\mathcal{O}}_3) + S(A) \\ &\quad - [\mathcal{I}(\hat{\mathcal{O}}_1 : B_1) + \mathcal{I}(\hat{\mathcal{O}}_3 : B_3)], \\ S(\hat{\mathcal{O}}_1|B_1) + S(\hat{\mathcal{O}}_4|B_4) &\geq -\log_2 c(\hat{\mathcal{O}}_1; \hat{\mathcal{O}}_4) + S(A) \\ &\quad - [\mathcal{I}(\hat{\mathcal{O}}_1 : B_1) + \mathcal{I}(\hat{\mathcal{O}}_4 : B_4)], \\ &\vdots \\ S(\hat{\mathcal{O}}_{N-1}|B_{N-1}) + S(\hat{\mathcal{O}}_N|B_N) &\geq -\log_2 c(\hat{\mathcal{O}}_{N-1}; \hat{\mathcal{O}}_N) \\ &\quad + S(A) - [\mathcal{I}(\hat{\mathcal{O}}_{N-1} : B_{N-1}) + \mathcal{I}(\hat{\mathcal{O}}_N : B_N)]. \end{aligned} \quad [27]$$

Then, we sum the $N(N-1)/2$ inequalities and divide both sides of the summed inequality by $N-1$. As a result, we have

$$\begin{aligned} \sum_{i=1}^N S(\hat{\mathcal{O}}_i|B_i) &\geq -\frac{\sum_{i \neq j, i=1}^N \log_2 c(\hat{\mathcal{O}}_i; \hat{\mathcal{O}}_j)}{N-1} \\ &\quad + \frac{N}{2} S(A) - \sum_{i=1}^N \mathcal{I}(\hat{\mathcal{O}}_i : B_i). \end{aligned} \quad [28]$$

By virtue of Renes–Boileau's result in Eq [5], we can write $N(N-1)/2$ formulas for N -observable measurements and the $N+1$ -party system $\rho_{AB_1B_2B_3B_4\cdots B_N}$ and directly obtain

$$\sum_{i=1}^N S(\hat{\mathcal{O}}_i|B_i) \geq -\frac{\sum_{i \neq j, i=1}^N \log_2 c(\hat{\mathcal{O}}_i; \hat{\mathcal{O}}_j)}{N-1}. \quad [29]$$

Linking Eq. [28] with Eq. [29], we define $\Delta_N = \frac{N}{2} S(A) - \left[\sum_{i=1}^N \mathcal{I}(\hat{\mathcal{O}}_i : B_i) \right]$ and take the maximum between Δ_N and

zero, then we obtain the desired GEUR for multi-observable in multipartite systems as described in Eq. [8].

ACKNOWLEDGMENTS. This work is supported by the Innovation Program for Quantum Science and Technology (No. 2021ZD0301200), the National Natural Science Foundation of China (Nos. 12174370, 12174376, and 11821404), the Youth Innovation Promotion Association of Chinese Academy of Sciences (No. 2017492), the Fok Ying-Tung Education Foundation (No. 171007). D.W. acknowledges the support by the National Natural Science Foundation of China (Grant Nos. 12075001, 61601002 and 12175001), Key Research and Development Project of Anhui Province (Grant No. 2022b13020004), and the fund from CAS Key Laboratory of Quantum Information (Grant No. KQI201701). S.K. acknowledges the financial support by the National Science Foundation under award number 1955907.

1. W Heisenberg, Über den anschaulichen inhalt der quantentheoretischen kinematik und mechanik. *Z. Physik* **43**, 172–198 (1927).
2. EH Kennard, Zur quantenmechanik einfacher bewegungstypen. *Z. Physik* **44**, 326–352 (1927).
3. HP Robertson, The uncertainty principle. *Phys. Rev.* **34**, 163 (1929).
4. D Wang, F Ming, ML Hu, L Ye, Quantum-memory-assisted entropic uncertainty relations. *Annalen der Physik* **531**, 1900124 (2019).
5. D Deutsch, Uncertainty in quantum measurements. *Phys. Rev. Lett.* **50**, 631 (1983).
6. K Kraus, Complementary observables and uncertainty relations. *Phys. Rev. D* **35**, 3070 (1987).
7. H Maassen, JB Uffink, Generalized entropic uncertainty relations. *Phys. Rev. Lett.* **60**, 1103 (1988).
8. JM Renes, JC Boileau, Conjectured strong complementary information tradeoff. *Phys. Rev. Lett.* **103**, 020402 (2009).
9. M Berta, M Christandl, R Colbeck, JM Renes, R Renner, The uncertainty principle in the presence of quantum memory. *Nat. Phys.* **6**, 659 (2010).
10. F Adabi, S Salimi, S Haseli, Tightening the entropic uncertainty bound in the presence of quantum memory. *Phys. Rev. A* **93**, 062123 (2016).
11. Y Huang, Entanglement criteria via concave-function uncertainty relations. *Phys. Rev. A* **82**, 012355 (2010).
12. MH Partovi, Entanglement detection using majorization uncertainty bounds. *Phys. Rev. A* **86**, 022309 (2012).
13. D Wang, F Ming, XK Song, L Ye, JL Chen, Entropic uncertainty relation in neutrino oscillations. *Eur. Phys. J. C* **80**, 800 (2020).
14. G Vallone, DG Marangon, M Tomasin, P Villoresi, Quantum randomness certified by the uncertainty principle. *Phys. Rev. A* **90**, 052327 (2014).
15. J Schneeloch, CJ Broadbent, SP Walborn, EG Cavalcanti, JC Howell, Einstein-podolsky-rosen steering inequalities from entropic uncertainty relations. *Phys. Rev. A* **87**, 062103 (2013).
16. A Riccardi, C Macchiavello, L Maccone, Multipartite steering inequalities based on entropic uncertainty relations. *Phys. Rev. A* **97**, 052307 (2018).
17. T Kriváchy, F Fröwis, N Brunner, Tight steering inequalities from generalized entropic uncertainty relations. *Phys. Rev. A* **98**, 062111 (2018).
18. I Devetak, A Winter, Distillation of secret key and entanglement from quantum states. *Proc. Royal Soc. A* **461**, 207 (2004).
19. PJ Coles, M Berta, M Tomamichel, S Wehner, Entropic uncertainty relations and their applications. *Rev. Mod. Phys.* **89**, 015002 (2017).
20. M Christandl, R Knig, R Renner, Postselection technique for quantum channels with applications to quantum cryptography. *Phys. Rev. Lett.* **102**, 020504 (2009).
21. V Scarani, R Renner, Quantum cryptography with finite resources: Unconditional security bound for discrete-variable protocols with one-way postprocessing. *Phys. Rev. Lett.* **100**, 200501 (2008).
22. ML Hu, H Fan, Competition between quantum correlations in the quantum-memory-assisted entropic uncertainty relation. *Phys. Rev. A* **87**, 022314 (2013).
23. J Feng, YZ Zhang, MD Gould, H Fan, Entropic uncertainty relations under the relativistic motion. *Phys. Lett. B* **726**, 527 (2013).
24. ML Hu, H Fan, Quantum-memory-assisted entropic uncertainty principle, teleportation, and entanglement witness in structured reservoirs. *Phys. Rev. A* **86**, 032337 (2012).
25. ZY Xu, WL Yang, M Feng, Quantum-memory-assisted entropic uncertainty relation under noise. *Phys. Rev. A* **86**, 012113 (2012).
26. Y Lee, S Lee, Activation of the quantum capacity of gaussian channels. *Phys. Rev. A* **98**, 012326 (2018).
27. MN Chen, D Wang, L Ye, Characterization of dynamical measurement's uncertainty in a two-qubit system coupled with bosonic reservoirs. *Phys. Lett. A* **383**, 977 (2019).
28. YB Yao, D Wang, F Ming, L Ye, Dynamics of the measurement uncertainty in an open system and its controlling. *J. Phys. B: At. Mol. Opt. Phys.* **53**, 035501 (2020).
29. CF Li, JS Xu, XY Xu, K Li, GC Guo, Experimental investigation of the entanglement-assisted entropic uncertainty principle. *Nat. Phys.* **7**, 752–756 (2011).
30. R Prevedel, DR Hamel, R Colbeck, K Fisher, KJ Resch, Experimental investigation of the uncertainty principle in the presence of quantum memory and its application to witnessing entanglement. *Nat. Phys.* **7**, 757–761 (2011).
31. ZY Ding, et al., Experimental investigation of entropic uncertainty relations and coherence uncertainty relations. *Phys. Rev. A* **101**, 032101 (2020).
32. B Demirel, S Sponar, AA Abbott, C Branciard, Y Hasegawa, Experimental test of an entropic measurement uncertainty relation for arbitrary qubit observables. *New J. Phys.* **21**, 013038 (2019).
33. W Ma, et al., Experimental test of heisenberg's measurement uncertainty relation based on statistical distances. *Phys. Rev. Lett.* **116**, 160405 (2016).
34. S Liu, LZ Mu, H Fan, Entropic uncertainty relations for multiple measurements. *Phys. Rev. A* **91**, 042133 (2015).
35. BF Xie, et al., Optimized entropic uncertainty relations for multiple measurements. *Phys. Rev. A* **104**, 062204 (2021).
36. S Designolle, P Skrzypczyk, F Fröwis, N Brunner, Quantifying measurement incompatibility of mutually unbiased bases. *Phys. Rev. Lett.* **122**, 050402 (2019).
37. C Zhang, et al., Experimental greenberger-horne-zeilinger-type six-photon quantum nonlocality. *Phys. Rev. Lett.* **115**, 260402 (2015).
38. T Bodiya, LM Duan, Scalable generation of graph-state entanglement through realistic linear optics. *Phys. Rev. Lett.* **97**, 143601 (2006).
39. I Devetak, A Winter, Distillation of secret key and entanglement from quantum states. *Proc. Royal Soc. A* **461**, 207–235 (2005).